Lab on a Chip

RSC Publishing

PAPER

View Article Online
View Journal

On the free-space Gaussian beam coupling to droplet optical resonators

Cite this: DOI: 10.1039/c2lc41214d

Noha Gaber,[a] Maurine Malak,[a] Xichen Yuan,[a] Kim Ngoc Nguyen,[a] Philippe Basset,[a] Elodie Richalot,[b] Dan Angelescu[a] and Tarik Bourouina*[a]

Received 30th April 2012,
Accepted 27th November 2012

DOI: 10.1039/c2lc41214d

www.rsc.org/loc

In this paper, light coupling into droplet optical resonators by means of a free-space Gaussian beam (GB) is investigated through numerical simulations and experiments. This method is introduced as an alternative to previously reported methods based on coupling through tapered fibers or prisms. Though applicable to solid-state optical resonators, this method is investigated here in the context of optofluidics for preserving the integrity of the droplet shape and for facilitating the steps of alignment and light coupling. The glycerol droplet under study is supported by a super-hydrophobic surface, which consists of Teflon-coated nanostructured silicon, to provide the advantage of keeping the droplet at a specific location, while maintaining a nearly spherical shape. The effectiveness of this method is tested with millimeter-sized droplets through measurements of their spectral responses. Quality factors Q in excess of 6×10^3 have been recorded. An analytical model for the external quality factor associated with this coupling technique has been derived, and the effect of the coupling parameters is demonstrated, allowing discussion about the scaling effects.

1. Introduction

Spherical optical resonators, either solid or liquid, have attracted high interest due to their symmetrical shape and their potential to sustain resonant whispering gallery modes (WGMs) with very high quality factors Q.[1–6] The quality factor, which is the primary figure of merit for optical resonators, describes the photon lifetime (τ_o) within the cavity, that is related to the optical losses of the system. WGMs can exhibit values of up to 10^{10} for the quality factor,[5,6] and thereby provide good optical resonators for many photonics applications such as lasing,[3] stimulated Raman scattering (SRS),[7–11] and passive filters.[5] In addition, the optical field is not completely confined, enabling it to interact and sense changes in the surrounding environment.[2] This renders microspheres suitable for chemical and biological sensing, with the added advantages of being label-free, and allowing affordable, fast, high-throughput measurements.[12] Detecting a single virus,[13] DNA,[2] or a single molecule,[5] have been reported in such systems.

For all these applications, high Q-factors are desired. In microspheres, limitations arise from several mechanisms like the dielectric material loss, scattering and inhomogeneity loss. These mechanisms govern the resonator's intrinsic (or internal) quality factor Q_{in} of the cavity itself. The overall quality factor, however, is also affected by the coupling (or external) quality factor Q_c, which needs to be maximized, rendering low-loss coupling methods essential. Ideally, besides offering a reasonable value for the coupling Q-factor, the coupling method should also be robust, flexible and repeatable, which is not the case for many of the conventional coupling methods reported,[14–17] especially when considering the *on-chip* coupling of light into spheres in the (sub-) millimeter diameter range. Thus, we propose coupling using a Gaussian Beam (GB) to harness the full benefit of using high-Q spherical resonators. It is worth mentioning that the technique of free-space coupling was thought initially to be inefficient for exciting the high-Q WGMs, which are supported by droplets that have a large radii compared to the exciting wavelength, since the radiation field tail of such modes is extremely small.[4] The technique was therefore limited to the scope of studying Mie resonances in aerosol microdroplets, and their elastic and inelastic scattering,[18,19] with very few practical applications. Furthermore, almost all the resonators considered were in the range of micrometers.[20–22] Free-space coupling to millimeter spheres by means of a GB has been insufficiently investigated, and to the best of our knowledge this paper is the first report of its implementation in a lab-on-chip environment, where its significant potential for analytical applications requires careful consideration.

Below, we explore the potential of the direct coupling of millimeter sized droplet optical resonators using a free-space Gaussian beam produced by a lensed optical fiber. This method has the advantages of avoiding physical contact

[a]Université Paris-Est, ESYCOM Lab., ESIEE Paris, 2 Bd. Blaise Pascal, 93162, Noisy-le-Grand, France. E-mail: t.bourouina@esiee.fr
[b]Université Paris-Est, ESYCOM Lab., UPEMLV, 5 Bd Descartes, 77454, Marne-la-Vallée, France

between the droplet and all micro-optical parts, thus facilitating the alignment process while preserving the integrity of the droplet, namely its composition and nearly spherical shape. The spherical shape is improved using a super-hydrophobic substrate called ''black-silicon'', a nanostructured silicon surface obtained by plasma processing at cryogenic temperatures.[23,24] Our demonstration is supported by numerical simulations of the electromagnetic field propagation, and by an analytical model for the calculation of coupling quality factors related to this coupling method.

2. Principle of free-space coupling through a Gaussian beam

There is a rich literature in the area of spherical resonators and different methods have been reported for coupling light to such resonators. Among the most widespread are those based on the use of prism couplers,[15,25–27] or tapered fibers.[1,16,28,29] Prisms and tapered fibers are two typical evanescent-field-based couplers. The prism couples light into the cavity through the evanescent field resulting from total internal reflection (TIR) while the tapered fiber couples light through the surrounding evanescent field at the vicinity of the fiber core surface. Each method has its advantages but neither can easily preserve the integrity of the liquid droplet shape while trying to produce significant coupling of the light inside the resonator. This requires a precise approach of the coupler at a distance in the order of 100 nm from the droplet surface, while avoiding physical contact that may lead to capillary effects and droplet collapse. In contrast, using a free-space Gaussian beam provides excellent control of the beam position with respect to the sphere resonator without the risk of capillary effects (Fig. 1 shows a schematic of the coupling setup). While previous uses of the method were limited to small microsphere sizes (for the studies related to light scattering), its implementation using millimeter and sub-millimeter sized droplets has very appealing characteristics: superior optical quality factors, ease of alignment and guaranteed droplet integrity.

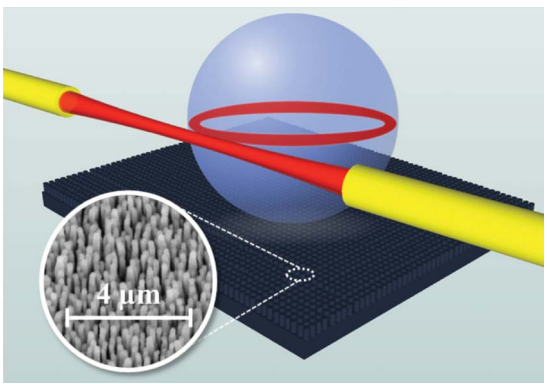

Fig. 1 Coupling using a free space Gaussian beam; the droplet is supported on a black silicon substrate, coated with Teflon. The inset is a scanning electron microscope image for the substrate.

3. Numerical simulations

To get a better idea about what may happen if a droplet is excited by a GB, simulations have been performed with the high frequency structural simulator (HFSS) software from ANSOFT, based on the finite element method (FEM). Though the simulations are performed on small-scale spheres, due to size limitations of the calculation domain, these simulation results provide a schematic representation of the field distribution involving coupling between a Gaussian beam and a WGM of a sphere resonator, as well as the resulting spectral response. Fig. 2 shows a sphere of radius 1.5 μm and a refractive index (n) of 1.47, excited by a GB, at wavelength λ = 1385 nm (at one of the resonances seen in the spectral response shown in Fig. 3). Due to the mirror symmetry of the structure, the simulation domain can be reduced to a hemisphere, improving the computation time.

Several positions for the GB optical axis placed at a distance S_0 from the sphere edge have been investigated. The field distributions show that when the GB axis is too far from the resonator (at a distance $S_0 = 4W_0$, where W_0 is the beam waist), no significant coupling could be seen, as shown in Fig. 2(a). However, significant coupling can be observed at $S_0 = 2W_0$, as indicated in Fig. 2(b), where the WGM excited inside the droplet can be recognized. Indeed, from this field distribution, the number of field maxima along the half circumference is 7, with a single maximum in the polar direction; hence it is

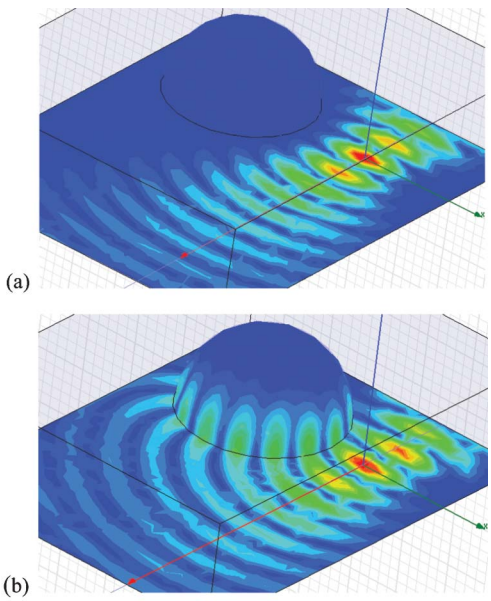

Fig. 2 Numerical simulations of a 1.5 μm droplet, n = 1.47 excited by a Gaussian beam as the optical axis is located at different distances S_0 expressed in units of the beam waist W_0:(a) $S_0 = 4W_0$; (b) $S_0 = 2W_0$, at resonant wavelength λ = 1385 nm of a whispering gallery mode.

identified as a fundamental mode with an angular mode order $\ell = 7$. The same value of the mode order is also evaluated for a similar radius-to-wavelength ratio using the characteristic equation of the WGM.[1]

The spectral transmission response for this droplet over a wavelength range from 1000 nm to 1600 nm has been obtained from numerical simulations, as indicated in Fig. 3, where the different resonances can be noticed including the resonance at $\lambda = 1385$ nm, whose mode shape is shown in Fig. 2(b).

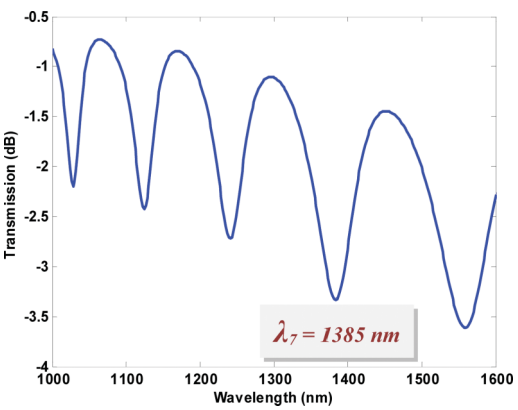

Fig. 3 Simulated spectral transmission response for a 1.5 μm radius droplet, n = 1.47 excited by a Gaussian beam located at distance $S_0 = 2W_0$. The 7th order resonance drop peak at λ = 1385 nm relates to the mode shape shown in Fig. 2(b).

4. Experimental results

4.1 Shape of glycerol droplets on a black silicon surface

For the sake of high quality factors, the sphericity of the droplet resonator is an important issue, especially in the equatorial region, to which the coupled wave is confined. Two effects are important to ensure nearly-perfect sphericity in the equatorial plane: the Bond number, and the contact angle of the droplet on the surface.

The Bond number $B_o = \rho g R^2/\sigma$ defines whether gravitational forces affect the droplet's spherical shape (ρ being the density of the fluid, g the gravitational acceleration, R the droplet radius, and σ its surface tension). In our case, $B_o < 0.4$ in all the experiments, implying very little deformation due to the droplet's own weight. The contact angle Θ on the substrate is a very important indicator of the equatorial sphericity as well: low contact angles lead to a highly deformed shape (possibly even without an equatorial plane if $\Theta < 90^\circ$), thus preventing the wave from resonating inside the cavity and leading to a very small quality factor Q. Ideally, a nearly-perfect spherical shape is desired, which is obtained for contact angles approaching 180°. In our experiments we used a Teflon-coated black silicon nanostructured surface to obtain high droplet contact angles, following prior reports that micro- and nano-structured silicon can exhibit super-hydrophobic surface characteristics.[30] Black silicon, consisting of needle-like

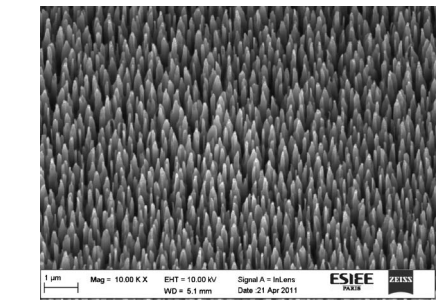

Fig. 4 SEM image of black Si obtained by a cryogenic DRIE process.

structures spaced 200 to 400 nm apart (SEM image in Fig. 4), is a material that is formed spontaneously during certain cryogenic plasma etching processes, and represents a cost-effective way of obtaining large-area nanostructured surfaces. Due to its light trapping capability and the resulting low reflectivity, such surfaces look black to the human eyes, hence their name of black silicon.[23,24]

Black silicon samples were obtained from p-type B-doped, (100) oriented, polished silicon wafers (resistivity 1–20 Ω·cm). The wafers were subjected to SF_6–O_2 plasma etching with a cryogenic process at −120 °C; such wafers were exposed to the plasma for about 10 min to obtain the required texture. SF_6 gas generates F* radicals for the chemical etching of silicon, leading to volatile SiF_4, whereas O_2 produces O* radicals leading to sidewall passivation with $Si_xO_yF_z$. Typical conditions of the inductively-coupled plasma were a power of 1000 W, a bias source of 30 V, and a chamber pressure of 1.5 Pa using an ALCATEL 601 system; the gases employed for the process were SF_6–O_2 (flow ratio of 20 : 1). After the black silicon formation step, the samples were exposed to a C_4F_8 plasma passivation step, which resulted in a 100 nm-thick Teflon-like layer deposited on the nanostructured black silicon substrate.

The liquid used to form the droplets was anhydrous glycerol (purity >99%, purchased from Merck Chemicals). The contact angles and the vertical and horizontal axis lengths were

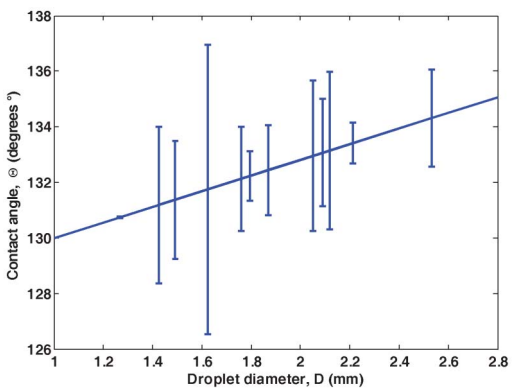

Fig. 5 Contact angle for different glycerol droplet sizes mounted on the black silicon substrate.

recorded from side-view images. Fig. 5 represents the contact angle *versus* the droplet diameter. It slightly increases with the droplet size, but maintains values larger than 130° throughout the experiments, within a suitable range to support WGM resonances in the equatorial plane.

Fig. 6(a) shows the effect of increasing droplet size on its sphericity, represented as the ratio between the double upper half lengths of the vertical axis ($2H$) over the droplet diameter (D). As the ratio is less than 100%, the droplets have a slight pancake-like deformation, which increases with the droplet size as expected. Nevertheless, the horizontal equatorial plan can still provide a nearly perfect circle, as can be seen in Fig. 6(b), which shows top view images for the glycerol droplets in the two extreme cases considered in the study of droplet sphericity: 1.27 mm and 2.53 mm diameters. The diameter is visibly the same for both the vertical and the horizontal axes of the photo, which indicates a circular path capable of attaining high quality factors for a wave successfully confined within the equatorial plane, or within its neighborhood.

4.2 Experimental validation of WGM excitation

An optical setup for injecting the Gaussian beam into a glycerol droplet and measuring the spectral response has been prepared for testing the proposed coupling method. The input light is produced by a source covering the near infrared wavelength range around λ = 1550 nm, injected and collected through single mode lensed fibers with beam waist radii of 9 or 25 μm. The near-infrared (NIR) is our spectral range of interest, but the visible red light used for alignment purposes

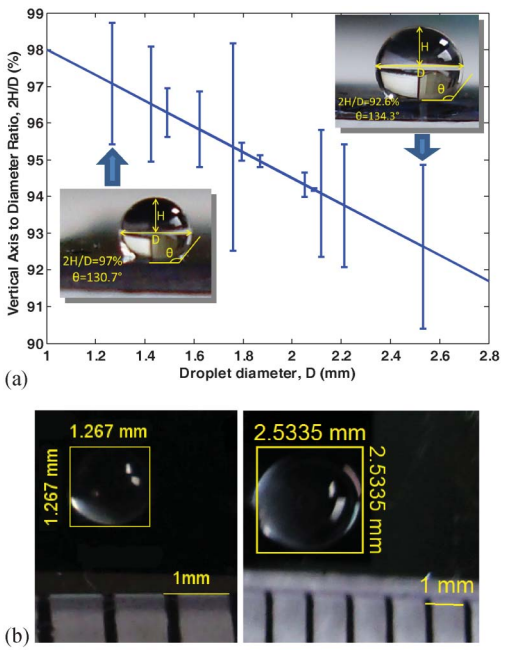

Fig. 6 (a) Shape ratio for different glycerol droplet sizes mounted on the black silicon substrate. The two insets are images of the droplet in the two extreme cases, indicating the axes ratio and the contact angle geometry. (b) Top view for the glycerol droplets in the smallest and the largest size, which indicates a circular path in the equatorial plane.

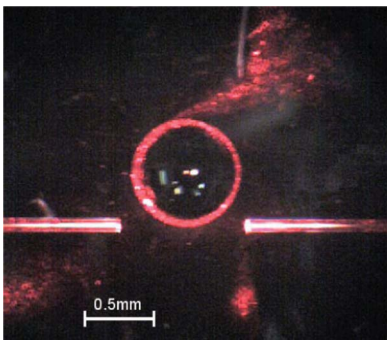

Fig. 7 Experimental demonstration of whispering gallery mode excited by a Gaussian beam using a set of lensed fibers having a beam waist radius of 25 μm, within a glycerol droplet that has a diameter of about 0.86 mm. Although measurements were performed using infrared light; visible in the figure is light from a secondary red laser used for alignment.

can also be coupled into the resonator, as shown in Fig. 7, which allows visualization of the WGM circulating near the perimeter edge of the sphere as a red ring. The transmitted light intensity is recorded using an optical spectrum analyzer. Fast Fourier transform (FFT) is applied to the data recorded from the measured spectrum to verify our observations.

Glycerol droplets with different diameters were mounted on the Teflon-coated black silicon substrates to achieve high contact angles. Glycerol is chosen for this kind of experiment due to its polarity (ensuring large contact angles on the super-hydrophobic black silicon surface), high viscosity (limiting droplet shape deformations due to thermal fluctuations and air currents), and to its low vapor pressure (less than 0.1 Pa at 20 °C, thus avoiding droplet size variation through evaporation over the duration of the experiment). The generated droplets' radii were in the range of hundreds of micrometers; droplets of this size may be subjected to residual torques and undergo rotation, if they were levitated, for instance by means of an acoustic levitator.[21] This was avoided by confining them to the black silicon surface, as droplets created by flowing glycerol through small syringe needles. All the experiments have been done in normal room conditions as far as temperature and humidity are concerned.

The spectral response corresponding to the input light wavelength range is recorded for droplets with diameters of about 0.78 and 1.16 mm. Due to the selective coupling of the resonant modes into the resonator, the response exhibits drops at certain wavelengths, as shown in Fig. 8. The quality factor depends on the droplet size, and it increases as expected with its diameter, as can be noted from comparing the values in Fig. 8(a), and 8(b). In the range of sizes studied, quality factors from 3.9×10^3 (for the 0.78 mm droplet) to 6.7×10^3 (for the 1.16 mm one) could be reached. As can be noticed from Fig. 9, which shows the FFT for the spectrum in Fig. 8(b), an optical path length of 5.36 mm gives a droplet diameter of 1.16 mm, noting that the glycerol has a refractive index n of 1.47. This is nearly the same diameter value measured from magnified images of the droplet.

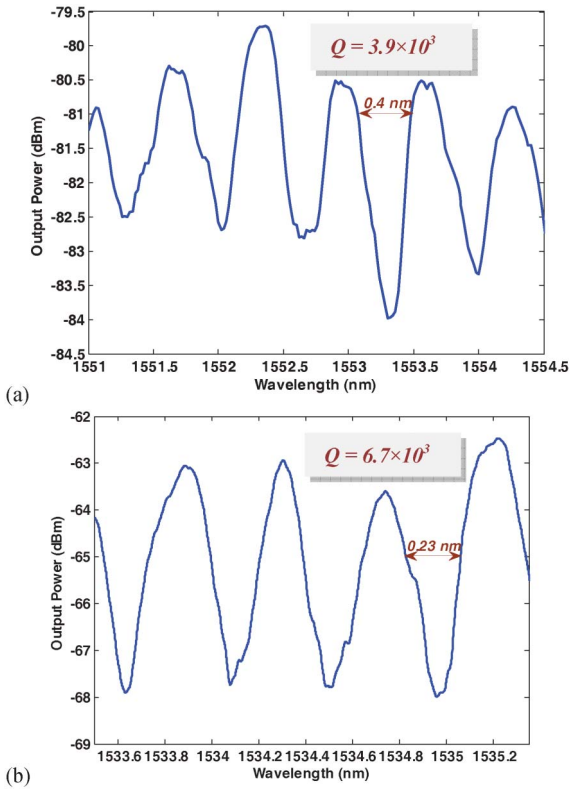

Fig. 8 Output power spectrum for: (a) a 0.78 mm diameter droplet. (b) a 1.16 mm diameter droplet, excited by a Gaussian beam with a beam waist radius of 9 μm. The 3 dB bandwidths are 0.4 and 0.23 nm, achieving total quality factors of 3.9×10^3 and 6.7×10^3 respectively.

5. Discussion

5.1 Micro-droplets *versus* millimeter droplets

In our work we adopt rather large, millimeter-size spheres (droplets), which differ from the micrometer-sized ones in several characteristics. The primary aspect is that, as the sphere size increases, the density of modes increases as well, and with it the principal number of resonances according to Mie theory,[31] and hence the mode's intrinsic quality factor or the radiative quality factors Q_{rad}. Therefore, increasing the diameter offers clear benefits in addition to easier production and handling. But on the other hand, the free space coupling was expected to become more difficult, and was even considered sometimes to be inefficient for exciting WGMs, as the radiative exchange of these modes with the external space is not sufficient when the radius exceeds several wavelengths.[4] More precisely, the highly confined WGMs, with radiative quality factors $Q_{rad} > 10^{20}$, possess negligible radiative losses, and hence are expected not to be accessible by free-space coupling like coupling using GB; therefore millimeter-sized droplets and even those with diameters in the hundreds of micrometers range were initially considered to require evanescent field coupling techniques.[25]

Another important difference between small and large sized droplet resonators is the validity of the van de Hulst's localization principle[31] that relates the principal mode number of the WGM to the external Gaussian beam position in order to obtain a maximized energy coupling to the spherical cavity mode. It states that a tightly focused Gaussian light beam passing outside but near a spherical microcavity will preferentially excite specific cavity modes, depending on its distance from the cavity center. But experimentally, it has been shown that this principle apparently fails because of surface perturbations in the low order modes, especially the first order, where most of the mode field is located near the surface; in such cases the optimal excitation position shifts to within the droplet, in disagreement with the Van de Hulst's principle. Hence, in droplets with radii larger than 20 μm, where there is a dramatic increase in the number of surface-limited modes, the van de Hulst localization principle is not expected to play an important role.[21]

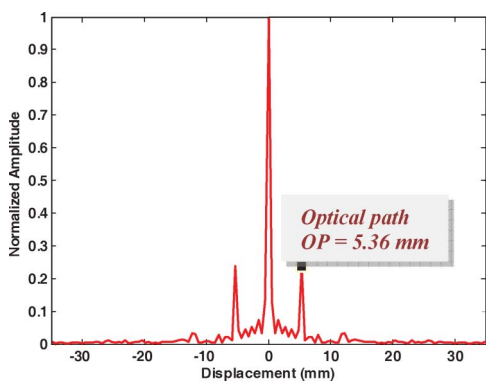

Fig. 9 FFT of the spectral response for a 1.16 mm diameter droplet.

5.2 Quality factor considerations

The quality factor is affected by losses in the system, some of which come from the resonator itself. Those internal losses set a certain internal quality factor Q_{in} for that resonator: ${Q_{in}}^{-1} = {Q_{rad}}^{-1} + {Q_{ss}}^{-1} + {Q_{cont}}^{-1} + {Q_{mat}}^{-1}$, where ${Q_{rad}}^{-1}$ denotes radiative losses of the WGM due to the curvature of the spherical guiding boundaries in the direction of propagation; ${Q_{ss}}^{-1}$, the scattering losses on the surface inhomogeneity; ${Q_{cont}}^{-1}$, losses introduced by surface contaminants; and ${Q_{mat}}^{-1}$, the material losses.[6] On the other hand, the loss due to coupling the light to the resonator sets a certain external or coupling quality factor Q_c. The total quality factor Q_{total} depends on both the intrinsic and coupling quality factors:[15,25,32] ${Q_{total}}^{-1} = {Q_c}^{-1} + {Q_{in}}^{-1}$ and is smaller than either one. Hence, we have different coupling regimes depending on the dominating loss processes. The coupling regime can be identified as under-coupled ($Q_{in} < Q_c$), critically coupled ($Q_c = Q_{in} = 2Q_{total}$) or over-coupled ($Q_{in} > Q_c$). At small radii microspheres, the radiation quality factor Q_{rad} is small and hence it is dominant, as the whispering gallery mode radiation loss is high due to the large curvature in the resonator. But it increases very quickly as the sphere size increases until it becomes ineffective at radii in the range of few tens of micrometers and more.[1,6] So, for millimeter diameter spheres, the overall quality factor is limited by either the coupling loss or the material and/or scattering losses.

In our case, we believe that the limit arises from the material loss. The coupling quality factor estimation gives extremely high-Q values ($Q_c > 10^{17}$), as will be demonstrated in the following section. While glycerol is a very suitable candidate for our experiment since its viscosity is high, its evaporation rate is low, and its contact angle to the substrate is relatively large, but it possesses non-negligible absorption in the NIR range, with an absorption coefficient α of about 1.1 to 1.36 mm^{-1} at wavelengths from 1530 to 1570 nm,[33] which limits the material quality factor Q_{mat} to about 5.5×10^3 if estimated by the bulk losses as $Q_{mat} = 2\pi n/\alpha\lambda$. This value may actually be slightly higher due to the bulk scattering loss suppression that takes place in microspheres, if we take into consideration the modifications in deriving the attenuation for closed resonant circulating waves such as WGMs from that of plane waves in the bulk medium.[34]

5.3 Coupling quality factor

As we have seen, the total quality factor Q_{total} is governed by intrinsic and coupling quality factors. Precise analysis of the contribution of each Q component is important. While it is essential to have sufficient coupling inside the droplet to excite the modes, trapped photons tend to leave the resonator sooner as the coupling is increased, thus increasing the losses and decreasing Q_c.[32] Hence, we set a model for calculating Q_c in the case of coupling light into a sphere with radius R_0 by means of a GB of half beam waist radius W_0. The corresponding key equations can be found in the appendix. Fig. 10 shows a schematic for the cross-sectional view of our system geometry when the Gaussian beam waist is located at the droplet edge.

Different parameters that may affect the coupling are illustrated, like the separation distance S_0 between the resonator and the beam, the sphere radius R_0, the refractive index of the resonator's material n_s. The derived formula for Q_c is used to examine the effect of these parameters. Among the coupling conditions, the most effective parameter is the separation distance S_0 between the resonator and the beam. If it is too large, there might be no coupling at all, as demonstrated in Fig. 2(a); if it is too close (less than about $1.5*W_0$), the GB may get deformed with significant coupling to the sphere. In Fig. 11, the behavior of the coupling quality factor Q_c is calculated for a GB whose beam waist radius W_0 is 9 μm, exciting droplets of radii 390 and 580 μm as they are moved away from the beam axis, starting from $1.5*W_0$ to $2.5*W_0$. One can first notice that Q_c increases due to the decreasing of the coupling strength as the resonator is moved away from the beam. Also it is apparent that larger droplet radii may lead to lager quality factors. Note that changing the material refractive index has the same effect of changing the radius as the optical path length is the multiplication of both the physical length and the refractive index. One can also notice from Fig. 11 extremely high values of Q_c, in excess of 10^{17}, which suggest that the coupling conditions will not be the limiting factor, as long as the intrinsic quality factor does not reach such levels. This is actually the case for the resonator's dimensions under consideration in this study. Indeed, for a 1.5 μm radius droplet, Q_c is typically about 10^{23}, but this is no use since the total quality factor is limited by a Q_{rad} of only 10, calculated from the whispering gallery intrinsic loss expresion[1] (dominated in this case by radiation losses). For a 1 mm radius droplet, Q_c is about 10^{16}, still leaving enough margin to excite resonant modes of very high quality factors. It is worth mentioning that the extremely high values of Q_c found through this study also suggest that in principle, the coupling method through Gaussian beams might be suitable for the measurement of very high quality factors, at least up to 10^{16}, as wide degrees-of-freedom are available in terms of coupling conditions and sphere dimensions.

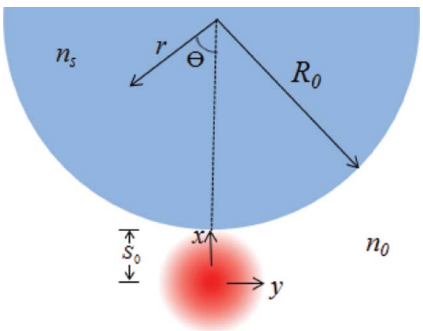

Fig. 10 Cross-sectional view of the geometry of the excitation Gaussian beam coupled to the sphere resonator.

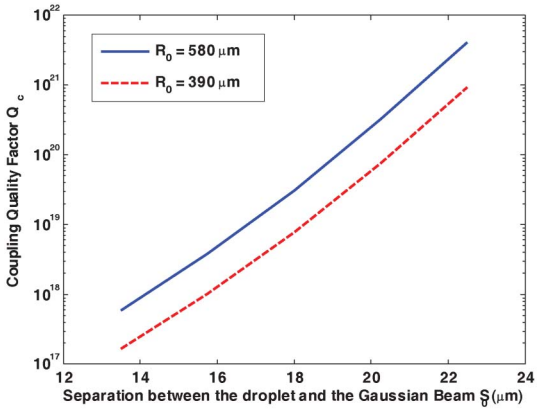

Fig. 11 Coupling quality factor Q_c at different separation distances S_0 for glycerol droplets of radii 580 and 390 μm; beam waist W_0 =9 μm.

6. Conclusion

The method for direct on-chip light coupling into millimeter-size droplet optical resonators using a free-space Gaussian beam has been validated and discussed. This method has many advantages over the conventional coupling methods like simplicity, easier coupling, low risk of collapsing the droplet resonator, and coupling distance adjustment in the range of microns.

Quality factors up to 6.7×10^3 were experimentally observed in the near infrared range, the main limitation being

internal material absorption. An analytical model for calculating the coupling quality factor in this method has been derived for the purpose of evaluating the ultimate limits of the proposed coupling method. The effects of the different types of losses on the total quality factor at the different coupling regimes and for different droplet sizes have been discussed. The effects of geometrical parameters on the coupling quality factor have also been analytically investigated. The proposed free-space coupling method can equally be used on non-absorbing liquid droplet resonators (in which case significantly higher quality factors can be expected due to the diminished absorption) as well as on solid-state spherical and disk resonators that exhibit much higher intrinsic quality factors.

Appendix: analytical expression for Gaussian beam coupling into a sphere resonator

Calculation of the coupling quality factor Q_c is derived here following the same steps as in ref. 1, but replacing the tapered fiber evanescent mode by a Gaussian beam of the following form[35]

$$U = A_0 \frac{W_0}{W(z)} e^{-\frac{\rho^2}{W^2(z)}} e^{-ikz - ik\frac{\rho^2}{2R(z)} - \xi(z)} \tag{1A}$$

The calculation steps are as follows: first we get the interaction strength $\kappa(S_0)$ at the point of minimum separation S_0 between the sphere and the beam. It is given by the overlap integral:

$$\kappa(S_0) = \frac{k}{2} \int_x \int_y \left(n_s^2 - n_0^2\right) U \Psi_{\ell,m,n} dx dy \tag{2A}$$

where $k = 2\pi/\lambda$ is the wave vector and $\Psi_{\ell,m,n}$ the field distributions the WGM resonating modes of orders ℓ,m,n.[1] Then, we integrate over the propagation coordinate z, taking into consideration that the separation S_0 now becomes $S(z)$. This integral is solved numerically in a region near the sphere edge. Once the coupling κ is obtained, one can accordingly calculate the coupling quality factor Q_c from $Q_c = m\pi/\kappa^2$. After a rigorous mathematical treatment, one finally obtains the coupling κ between the WGM in the regain near the equatorial plan (small θ angle) with a GB, in the following form:

$$\kappa = \frac{k}{2}\left(n_s^2 - n_0^2\right) N_s W_0 \frac{R_0}{\sqrt{m}} H_N(0) \int_z \frac{A_0(z)}{W(z)} \sqrt{\frac{2\pi}{q(z)+1}} \left|\frac{q(z)-1}{q(z)+1}\right|^{\frac{N}{2}}$$
$$\left[B\sqrt{\frac{\pi R_0^2}{2mq(z)}} \left(1 - erf\left(\sqrt{\frac{mq(z)}{2R_0^2}} S(z)\right)\right) \right. \tag{3A}$$
$$\left. - \frac{R_0^2}{mq(z)} . De^{-\frac{m}{2R_0^2} q(z).S^2(z)} \right] . e^{-i(\Delta\beta z - \xi(z))} dz$$

where:

$$B = (1+\ell) j_\ell(kn_s R_0) - R_0 kn_s j_{\ell+1}(kn_s R_0),$$
$$D = \frac{\ell}{R_0} j_\ell(kn_s R_0) - kn_s j_{\ell+1}(kn_s R_0),$$
$$\beta = \frac{\sqrt{\ell(\ell+1)}}{R_0},\ N = \ell - m$$
$$N_s = \left\{ \frac{\pi}{m} 2^{N-1} N! R_0^2 \left[\left(1 + \frac{1}{\alpha_s R_0}\right) j_\ell^2(kn_s R_0) \right.\right. \tag{4A}$$
$$\left.\left. - j_{\ell-1}(kn_s R_0) - j_{\ell+1}(kn_s R_0) \right] \right\}^{-1/2},$$
$$\alpha_s = \sqrt{\beta_\ell^2 - k^2 n_0^2},\ \Delta\beta = k_0 - \frac{m}{R_0}$$

References

1 B. E. Little, J. P. Laine and H. A. Haus, *J. Lightwave Technol.*, 1999, **17**, 704.
2 H. K. Hunta and A. M. Armani, *Nanoscale*, 2010, **2**, 1544.
3 M. Himmelhaus, *Opt. Commun.*, 2011, **284**, 4843.
4 A. B. Matsko and V. S. Ilchenko, *IEEE J. Sel. Top. Quantum Electron.*, 2006, **12**, 3.
5 V. S. Ilchenko and A. B. Matsko, *IEEE J. Sel. Top. Quantum Electron.*, 2006, **12**, 15.
6 M. L. Gorodetsky, A. A. Savchenkov and V. S. Ilchenko, *Opt. Lett.*, 1996, **21**, 453.
7 S. M. Spillane, T. J. Kippenberg and K. J. Vahala, *Nature*, 2002, **415**, 621.
8 A. Biswas, H. Latifi, R. L. Armstrong and R. G. Pinnick, *Phys. Rev. A: At., Mol., Opt. Phys.*, 1989, **40**, 7413.
9 R. Sharma, J. P. Mondia, J. Schäfer, Z. H. Lu and L. J. Wang, *J. Appl. Phys.*, 2009, **105**, 113104.
10 H. Taniguchi, H. Tomisawa and R. Nagashima, *Jpn. J. Appl. Phys.*, 1993, **32**, L1621.
11 A. Biswas, R. G. Pinnick, J. G. Xie, T. E. Ruekgauer and R. L. Armstrong, *Opt. Lett.*, 1992, **17**, 1569.
12 S. Selimovic and A. Khademhosseini, *Lab Chip*, 2012, **12**, 503.
13 F. Vollmer, S. Arnold and D. Keng, *Proc. Natl. Acad. Sci. U. S. A.*, 2008, **105**, 20701.
14 Y. F. Yu, T. Bourouina, C. S. Lim, M. K. Chin and A. Q. Liu, *μTAS2008*, San Diego, USA, p. 302.
15 Y. F. Yu, V. Kanna, T. Bourouina, S. H. Ng, P. H. Yap and A. Q. Liu, *IEEE Int. Conf. Micro Electro Mech. Syst., 23rd*, 2010, 831.
16 Y. F. Yu, T. Bourouina, S. H. Ng, P. H. Yap and A. Q. Liu, *μTAS2009*, Jeju, Korea, 979.
17 Y. F. Yu, T. Bourouina and A. Q. Liu, *Transducers'09*, 2009, 2011–2013.
18 P. W. Barber and R. K. Chang, *Optical Effects Associated with Small Particles*, World Scientific, Singapore, 1988.
19 R. K. Chang and Y.-L. Pan, *Faraday Discuss.*, 2008, **137**, 9.
20 E. E. M. Khaled, S. C. Hill, P. W. Barber and D.. Q. Chowdhury, *Appl. Opt.*, 1992, **31**, 1166.
21 H. B. Lin, J. D. Eversole and A. J. Campillo, *Opt. Lett.*, 1998, **23**, 1921.
22 R. M. Sayer, R. D. B. Gatherer, R. J. J. Gilham and J. P. Reid, *Phys. Chem. Chem. Phys.*, 2003, **5**, 3732.

23 K. N. Nguyen, D. Abi-Saab, P. Basset, E. Richalot, F. Marty, D. Angelescu, Y. Leprince-Wang and T. Bourouina, *Proc. 16th Int. Conf. Solid-State Sens., Actuators Microsyst., Transducers*, Beijing, China, 2011, 354.
24 K. N. Nguyen, D. Abi-Saab, P. Basset, E. Richalot, M. Malak, N. Pavy, F. Flourens, F. Marty, D. Angelescu, Y. Leprince-Wang and T. Bourouina, *Microsyst. Technol.*, 2012, DOI: 10.1007/s00542-012-1486-0.
25 M. L. Gorodetsky and V. S. Ilchenko, *J. Opt. Soc. Am. B*, 1999, **16**, 147.
26 S. Schiller and R. L. Byer, *Opt. Lett.*, 1991, **16**, 1138.
27 M. L. Gorodetsky and V.S. Ilchenko, *Opt. Commun.*, 1994, **113**, 133.
28 A. Chiba, H. Fujiwara, J.-I. Hotta, S. Takeuchi and K. Sasaki, *Appl. Phys. Lett.*, 2005, **86**, 261106.
29 S. M. Spillane, T. J. Kippenberg, O. J. Painter and K. J. Vahala, *Phys. Rev. Lett.*, 2003, **91**, 043902.
30 T. Baldacchini, J. E. Carey, M. Zhou and E. Mazur, *Langmuir*, 2006, **22**, 4917.
31 H. C. van de Hulst, *Light Scattering by Small Particles*, Dover Publications, New York, 1981.
32 F. Vanier, C. La Mela, A. Hayat and Y.-A. Peter, *Opt. Express*, 2011, **19**, 23544.
33 K. Izutsu, Y. Hiyama, C. Yomota and T. Kawanishi, *AAPS PharmSciTech*, 2009, **10**, 524.
34 M. L. Gorodetsky, A. D. Pryamikov and V. S. Ilchenko, *J. Opt. Soc. Am. B*, 2000, **17**, 1051.
35 B. E. A. Saleh and M. C. Teich, *Fundamentals of Photonics*, ch. 3, John Wiley & Sons, 1991.